

Optical anomalous Hall effect and the electrical detection of spin current in semiconductors

M. Idrish Miah

Department of Physics, University of Chittagong, Chittagong-4331, Bangladesh.

Abstract

We observed the optical anomalous Hall effect (AHE) and showed the optical AHE as a technique for the electrical detection of spin current in nonmagnetic semiconductors. As no external magnetic field was used, the effect was the pure AHE, i.e. without any contribution from the ordinary Hall current. The optical pure AHE originated from non-equilibrium magnetization induced by spin-polarized electrons generated by the circularly polarized light. A strong bias-field dependence of the optical AHE was observed. It was however demonstrated that when the electron spins were dragged with a high field a very significant decrease was occurred in the spin polarization due to an increase in the spin precession frequency of the hot electrons. The optical AHE was also found to strongly depend on the pumping photon energy, which might be due to the photon energy-dependent inter-band filling. The results were discussed based on the dominating spin relaxation mechanism.

Keywords: Spin current; Anomalous Hall effect; Spin relaxation; Semiconductor

1. Introduction

Spintronics refers to the study of the role played by electron spin in solid state physics, and possible devices of increased capability and functionality, such as spin field-effect transistors, spin storage/memory devices or spin quantum computers, that specifically exploit spin properties instead of, or in addition to, charge degree of freedom [1-3]. The idea to use the spin property of electrons in conventional electronic devices has drawn a lot of attention recently [3-6], motivated by the observations of long spin lifetime (τ_s), or spin diffusion length [7,8], and high spin-polarization [9] in semiconductors.

However, one of the important requirements necessary in developing semiconductor spintronic devices is the detection of spin current in a semiconductor [3,5]. The detection of spin current in semiconductors has been obtained mostly by optical methods [2,10,11]. However, an electrical means of detecting spin current in semiconductors

is desirable for possible device applications. It has recently been proposed that the anomalous Hall effect (AHE) could be used as a technique for the electrical detection of spin current in semiconductors [12]. The AHE has also attracted much attention because of its close theoretical connection to the spin Hall Effect (a transverse spin current following in response to an applied electric field in the presence of spin-orbit interaction) [13] and because of the rapidly growing interest in spin-dependent transport phenomena [6,14]. In addition, the AHE has been used in demonstrating the existence of a ferromagnetic state in several semimagnetic (diluted magnetic) semiconductors while searching for materials for possible applications in spintronics.

The properly understanding of the AHE, that is of that part of the transverse resistance which depends on the magnetization, is still a challenging problem in semiconductors. However, it has been generally recognized that the spin-orbit

interaction is responsible for the effect, and due to this interaction, electrons with their spin polarization parallel to the magnetization axis will be deflected at right angles to the directions of the longitudinal electric current and of the magnetization while electrons with antiparallel spin polarization will be deflected in the opposite direction via the skew-scattering (SS) and side-jump (SJ) [15]. Thus, if the two spin species (spin-up and spin-down) are unequal, there appears a net current in the transverse direction.

In the ordinary Hall effect (HE), the Lorentz force (F) causes a charge imbalance by deflecting like-charge carriers towards one boundary of the sample (Fig. 1), creating a voltage transverse to the applied electric and magnetic fields. The AHE is the result of spin-dependent deflection of carrier (spin-polarized) motion, which produces a Hall voltage proportional to the spin polarization (or the magnetization) and a spin accumulation at the transverse boundaries. In the AHE, the spin-orbit interaction plays the role of the force, so-called spin-orbit coupling force (F_{SO}), that deflects like-spin carriers to one boundary and opposite spins to the other boundary, which causes a spin imbalance as well as a charge imbalance and results in a transverse Hall voltage (AHE voltage).

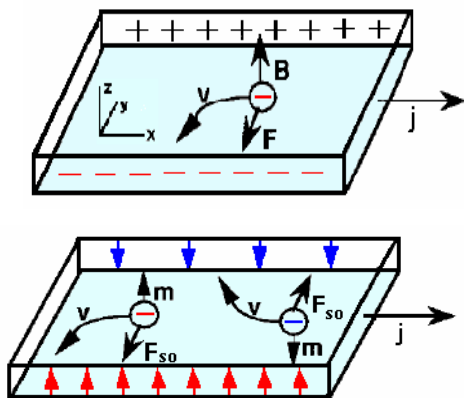


Fig. 1. (Top) Hall effect with the application of an external magnetic field, \mathbf{B} and (Bottom) anomalous Hall effect (AHE). In the AHE, carriers with same charge but opposite spin are deflected (in the presence of the magnetization, \mathbf{m}) by the spin-orbit coupling to opposite sides of the sample.

The AHE in magnetic materials with the application of magnetic fields has been observed for a long time since its discovery in 1880 by Hall. The total Hall resistivity (ρ_H) of the magnetic

materials in the presence of magnetic fields can be expressed [15] as a sum of two terms:

$$\rho(B) = \rho_H(m) + \rho_{AH}(B) = R_H B + 4\pi R_{AH} m \quad (1)$$

(in cgs units), where is $R_H = (en_s)^{-1}$ is the ordinary Hall coefficient and R_{AH} the anomalous Hall coefficient. The first term (the ordinary Hall resistivity, $\rho_H = R_H B$) is due to the Lorentz force acting on the charge carriers and is present in nonmagnetic materials as well and is proportional to the magnetic field B , and inversely proportional to the charge per carrier (e) and the sheet density of carriers (n_s). The second term ($\rho_{AH} = 4\pi R_{AH} m$) is the anomalous contribution and is a characteristic of the magnetic state of the material and is proportional to the magnetization (m). Thus, the AHE observed in magnetic materials is not pure, but a mixture of HE (as a major component) and AHE.

As mentioned earlier, two different spin-dependent scattering mechanisms (i.e. asymmetries in scattering for up- and down-spins) are responsible for AHE or R_{AH} [15]. They are the classical asymmetric SS (amplitude of the scattered wave packet becomes anisotropic) and the nonclassical SJ (charge carrier changes its trajectory because of a lateral displacement) mechanisms, both having their origin in the spin-orbit interaction present in a ferromagnet or magnetic material. The AHE coefficient R_{AH} is described by

$$R_{AH} = \alpha_c \rho_l|_{SS} + \beta_c \rho_l^2|_{SJ}, \quad (2)$$

where ρ_l is the longitudinal resistivity and α_c and β_c are constants. The linear and quadratic terms in Eq. (2) are the SS and the SJ contributions, respectively. However, it has recently been predicted that there is another contribution, called the intrinsic contribution, which is not related to scattering, but arising as a result of the band structure [5]. So, the evaluation of the intrinsic contribution does not require knowledge of the disorder or impurity present in the system.

While the HE results from the Lorentz force, AHE is due to the spin-orbit coupling in the present of spin polarization (i.e. the imbalance in the population of carriers with \uparrow and \downarrow spins) or magnetization m . In a ferromagnetic metal, the presence of the spontaneous m leads to AHE. For a nonmagnetic semiconductor, there is no spontaneous m , so one needs to apply a magnetic

field to polarize the carriers, and the effect consists of two contributions: the ordinary one and an AHE, as in ferromagnetic or magnetic materials. The spin-dependent Hall effect (like AHE) observed in *n*-doped InSb and Ge has been separated from the much larger ordinary Hall effect by using a spin-resonance method [16]. If one, however, can generate a spin current (unequal spin populations) into a semiconductor such that it can be sustained on the required length (or time) scale, one could observe AHE. In the presence of the generated spin currents, the nonmagnetic semiconductor could behave more like a ferromagnet as far as or as long as the transport is concerned.

Here in the present investigation, we fabricate nonmagnetic semiconductor devices and polarize the electron spins in the devices by a circularly polarized light to generate a spin-polarized current (or spin current) for the induction of nonequilibrium magnetization and the observation of optical AHE [17]. As the present experiment is performed without external magnetic fields or ferromagnetic couplings, the devices measured the optically induced pure anomalous Hall current,

$$\rho(B=0) = \rho_{AH} = 4\pi R_{AH} m, \quad (3)$$

i.e. without any contribution from the ordinary Hall current ($\rho_H = R_H B = 0$). The optical pure AHE as a function of the longitudinal electric field and excitation photon energy are measured. It is demonstrated that the optical AHE can be used as a technique for the electrical detection of spin current in nonmagnetic semiconductors. The results are discussed based on the Dyakonov–Perel (DP) [18,19] spin relaxation mechanism.

2. Spin current generation

A spin-polarized carrier population can be generated by the absorption of a monochromatic right (left) circularly polarized light σ^+ (σ^-) pulse with appropriate photon energy in a bulk semiconductor, such as GaAs [20]. In optical pumping, circularly polarized photons transfer their angular momenta to electrons for the unequal spin [spin-up (\uparrow) and spin-down (\downarrow)] populations (spin polarization) or the induction of a net magnetization. In GaAs, the conduction band (*s*-symmetry) is twofold degenerate at the centre of the Brillouin zone ($\vec{k} = 0$), corresponding to spin-up and spin-down electrons ($m_j = \pm 1/2$). The

valence band (*p*-symmetry) at $\vec{k} = 0$ is split by spin-orbit interaction into heavy-hole (HH) and light-hole (LH) bands and a split-off band (SO). The HH and LH bands, with large and small effective masses, are each twofold spin degenerate ($m_j = \pm 3/2, \pm 1/2$). The production of a carrier population with a net spin (unequal spin populations) by direct absorption of a circularly polarized light is a consequence of the optical selection rules [$\Delta m_j = +1$ ($\Delta m_j = -1$) for right (left) or σ^+ (σ^-)] for the HH and LH valence to conduction band transitions. The strengths of the optical inter-band valence to conduction band transitions are given by the inter-band matrix transition dipole elements for the HH, LH and SO bands and are 3: 1: 2, respectively (Fig. 2). Pumping with a σ^- (σ^+) of both HH and LH transitions in unstrained bulk GaAs yields an initial spin polarization, defined as

$$p(\vec{r}, t) = \frac{n_{\uparrow}(\vec{r}, t) - n_{\downarrow}(\vec{r}, t)}{n_{\uparrow}(\vec{r}, t) + n_{\downarrow}(\vec{r}, t)}, \quad (4)$$

of $p(0,0) = +0.5(-0.5)$ (50%), since the inter-band transition dipole matrix elements of the HH transition are three times stronger than those of the LH transitions. Here $n_{\uparrow}(n_{\downarrow})$ is the density of spin-

up (spin-down) electrons. Optical pumping with σ^- (σ^+) generates spins along the direction antiparallel (parallel) to the direction of the light propagation, i.e. spins along $+z$ ($-z$) (Fig. 1).

Since optically pumping hole spin relaxation is extremely fast (≤ 100 fs), their polarization is effectively zero and need not be considered [3]. Pumping with energies equal to or larger than the SO band transition yields no electron spin polarization, since LH and SO band transitions create the same electron spin orientation and the sum of their inter-band matrix elements is equal to the HH inter-band dipole transition matrix element. Unequal spin populations, i.e. spin-polarized electrons in GaAs can thus be produced by the optical pumping (absorption) of a circularly polarized light pulse with photon energy above the direct band gap (E_g) but low enough to avoid exciting carriers from the SO band to the conduction band. A spin-polarized carrier population produced in this way will be distributed symmetrically in *k*-space in materials with zinc-blende symmetry and, consequently, there can be no net electrical current without a dc-bias field, even though each individual carrier may be

generated initially with a large momentum when the material is excited well above the band gap.

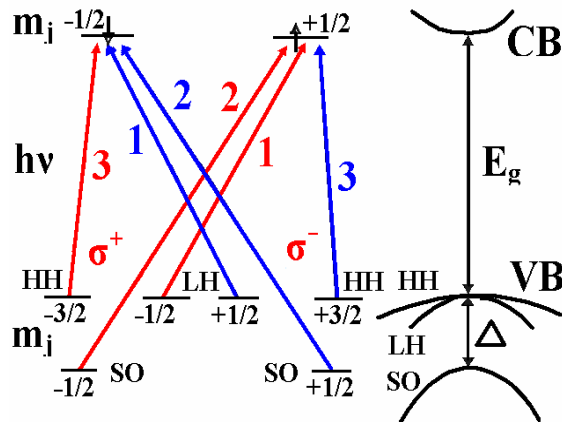


Fig. 2. Optical selection rules for the transitions from the heavy-hole (HH), light-hole (LH) and split-off (SO) valence bands (VB) to conduction band (CB). The allowed transitions for σ^+ ($\Delta m_j = +1$) and σ^- ($\Delta m_j = -1$) are shown by the red and green lines respectively, where σ^+ (σ^-) is for right(left) circularly polarized light. The numbers near the lines represent the relative transition probabilities. On the right, an E vs. k diagram of the energy bands of GaAs at $k=0$ shows the energy gap (E_g) and the spin-orbit splitting (Δ) of the valence bands. The degenerate states (energy levels) at $k=0$ are labelled on the left by their m_j quantum numbers. The small up (\uparrow) and down arrows in CB indicate the electron's spin orientation.

Optically generated spin-polarized carrier populations have recently been dragged by an external electric field to create a spin-polarized electrical current or spin current [3]. The longitudinal charge current of such a system is spin-polarized, i.e. the current of spin-up (\uparrow) electrons (J_{\uparrow}) is not equal to the spin-down current (J_{\downarrow}), although both species of electrons move in the same direction, which gives a non-zero spin current (J_s) flowing in the transverse direction (along y):

$$J_s(\vec{r}, t) \equiv J_{\uparrow}(\vec{r}, t) - J_{\downarrow}(\vec{r}, t), \quad (5)$$

where $J(\vec{r}, t) = J_{\uparrow}(\vec{r}, t) + J_{\downarrow}(\vec{r}, t)$ is the total longitudinal charge current.

3. Experimental

The investigated devices were fabricated on n -type ($2 \times 10^{16} \text{ cm}^{-3}$) GaAs. Four Au/Ge/Pd contacts in Hall geometry (with spacing $10 \mu\text{m} \times 20 \mu\text{m}$; $10 \mu\text{m}$ between Hall probes) were deposited on the substrates, with Pd layers adjacent to the GaAs substrates, using an e-beam evaporator with a base pressure of $\sim 5 \times 10^{-8}$ Torr. The contact metallization was annealed in a tube furnace in flowing nitrogen at temperature 180°C for 1 h to achieve ohmic contacts with low contact resistance. Contact formation details were reported elsewhere [21]. Gold wires were bonded from the sample-holder to the contact pads. For optical pumping, a mode-locked Ti:sapphire laser which generates ps pulses at 76 MHz repetition rate was used. The pumping photon energy $E_{\lambda} = hc/\lambda$ was varied for the measurements of its dependence. The wavelength of the light beam was measured using a wavelength meter. A neutral density wheel (Filter, F) was used to vary the optical power level. The average power on the sample was ~ 5 mW. The polarization of the optical beam was modulated using a photo-elastic modulator (PEM) at lock-in reference frequency of 42 kHz. The laser beam was focused to a $\sim 9 \mu\text{m}$ (FWHM) spot of the sample with a lens (L) with focal length $f=12$ cm. Measurements were performed at liquid helium temperature. Care was taken not to illuminate any of the electrical contacts to avoid the generation of any artefacts. To check that the beam hits the sample on the desired location, a microscope was used. The lens was designed for minimum spherical aberrations. The spot size was measured by knife-edge scans and the spatial (or the sequence focus) profile of the pulse was found to be Gaussian. A regulated electric power supply was used as a bias source. The signal was measured by a lock-in amplifier (signal detector, SD) coupled to a computer. A schema of the experimental setup is shown in Fig. 3.

4. Results and discussion

The spin-orbit coupling in a nonmagnetic semiconductor produces left-right asymmetric scattering of the carriers for a fixed spin orientation. The spin-up electrons, for example, tend to be scattered to the right more than to the

left via SS and SJ. If the longitudinal current is spin-polarized, e.g. current carriers contain more spin-up electrons than spin-down electrons, there would be more electrons scattered to the right than to the left.

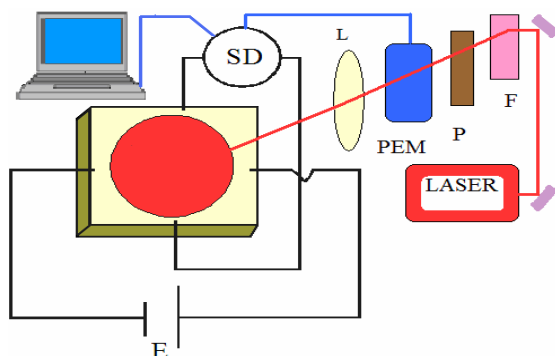


Fig. 3. A schema of the experimental setup for spin current detection in a nonmagnetic semiconductor device, based on the measurement of optical AHE (P: Polarizer, SD: Signal detector and E: Bias field).

This leads to both spin and charge accumulations in the transverse direction of the sample. The Hall (AHE) voltage is precisely the measure of this net charge accumulation and is proportional to the spin current in nonmagnetic materials. Since the photo-generated hole spins relaxation is extremely fast [3], the experiment observes only the effect resulting from spin-polarized electrons accumulating at the transverse boundaries of the sample, as a result of left-right asymmetries in scattering for spin-up and spin-down electrons in the presence of spin-orbit interaction.

The results obtained from the experiments are presented in Figs. 4 and 5. In Fig. 4, we show a typical signal at bias-field of $120 \text{ mV } \mu\text{m}^{-1}$ and photon energy of $E_{\lambda}=1.7 \text{ eV}$ (top). The lower curve shows the signal with an opposite sign when the accelerating field is reversed. The transverse voltage signal changes its sign with reversing the direction of the bias field. This is because the electron-spin polarization and thus the photo-induced magnetization direction change with the direction of the bias field.

In Fig. 5, we plot the optical V_{AHE} as a function pumping photon energy, where an average of the data taken from several experiments was calculated. As seen, there is a signal of $\sim 0.3 \mu\text{V}$ even at $E = 0 \text{ mV } \mu\text{m}^{-1}$ or for fields higher than $E = 400 \text{ mV } \mu\text{m}^{-1}$.

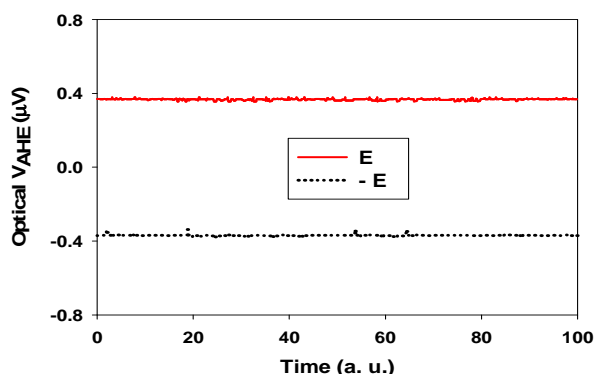


Fig. 4. A typical scan at bias-field of $120 \text{ mV } \mu\text{m}^{-1}$ and photon energy of $E_{\lambda}=1.7 \text{ eV}$ (Top). The lower curve shows the signal when the biased field is reversed.

This background signal is not due to a Hall current and cannot be related to AHE, since AHE does not occur at zero applied bias. We also observed the same background signal with illumination with linearly polarized light. Because our devices contained ohmic contacts, they measured the actual field accelerating the carriers, i.e. there was no chance that the measured voltage signal contained unwanted contributions. The background signal might be our PEM threshold.

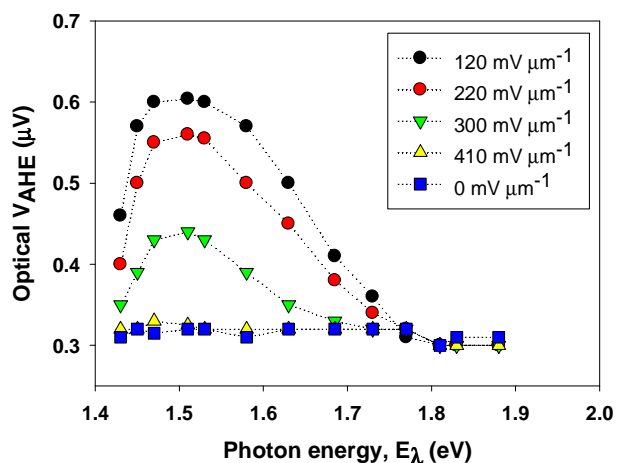


Fig. 5. Dependence of the signal on pumping photon energy and bias-field. An average of the data taken from several experiments for a field-strength was calculated.

As can be seen from the Fig. 5, the signal strongly depends on the pumping photon energy E_λ and for the excess photon energy $\Delta E_\lambda = E_\lambda - E_g$ within the range 50–120 meV, the sample gives the maximum value of optical V_{AHE} . With the further increase in energy, V_{AHE} decreases and finally reduces to the background for ~ 340 meV, which is the spin-orbit splitting energy Δ (Fig. 2). This might be because of exciting carriers from the SO band. The photon energy dependent band-filling effect has been discussed in details in Ref. [22]

Above $E = 150 \text{ mV } \mu\text{m}^{-1}$, the optical V_{AHE} was found to decay, and it disappeared for high fields. The decay of optical V_{AHE} with E might be due to the enhanced electron spin relaxation at higher current densities. As found, the photo-generated spin can travel without losing their initial orientation as long as their field is below a threshold value. Above the threshold $E_0 = 150 \text{ mV } \mu\text{m}^{-1}$ ($E > E_0$), spin depolarization is considerably enhanced due to the enhanced spin relaxation as a result of increase of the electron temperature (T_e). Our results agree with those of the bias-dependent spin transport experiment by Hägele *et al.* [23]. These authors studied spin relaxation of photo-generated electrons during drift transport in GaAs at low temperatures by photoluminescence measurements. They found almost complete conservation of the orientation of the electron spin during transport in GaAs over a distance as long as $4 \mu\text{m}$, but fields up to a couple of hundreds $\text{mV } \mu\text{m}^{-1}$. The results obtained by us are also in good agreement with those of the spin transport experiments performed by Sanada *et al.* [24], similar to one employed in [23]. They showed that the photo-generated spins could travel without losing their initial spin orientation as long as E was below $100 \text{ mV } \mu\text{m}^{-1}$ and the spin relaxation rate increased rapidly with E , and polarization disappeared at $\sim 350 \text{ mV } \mu\text{m}^{-1}$. It is noted that the spins in their study were generated with a higher optical power. The results are also consistent with those observed in the band-structure calculations using norm-conserving pseudopotential and Green function methods [25].

The origin of field-dependent efficient electron spin relaxation is discussed based on the DP spin relaxation mechanism [18,19]. The DP mechanism is due to spin-orbit coupling in semiconductors lacking inversion symmetry. In III-V semiconductors, such as GaAs, the degeneracy in the conduction band is lifted for $\vec{k} \neq 0$ due to the absence of inversion symmetry. Without inversion symmetry the momentum states of \uparrow and \downarrow spin

electrons are not degenerate, i.e. $E_{\vec{k}\uparrow} \neq E_{\vec{k}\downarrow}$, where $E_{\vec{k}\uparrow}(E_{\vec{k}\downarrow})$ is the momentum-dependent electron energy with spin $\uparrow(\downarrow)$. The resulting energy difference, for electrons with the same \vec{k} but different spin states, plays the role of a wave vector \vec{k} -dependent intrinsic magnetic field [26], $\vec{h}(\vec{k}) = \alpha \hbar^2 (2emE_g)^{-1/2} [k_x(k_y^2 - k_z^2)\hat{x} + c.p.]$, where α is a dimensionless, material-specific parameter which gives the magnitude of the spin-orbit splitting and is approximately given by $\alpha \approx 4\eta(m/m_{cv})/\sqrt{3-\eta}$ (where $\eta = \Delta/(E_g + \Delta)$, E_g is the bandgap, Δ is the spin-orbit splitting of the valence band, m is the electron's effective mass and m_{cv} is a constant close in magnitude to free electron mass m_0) induced by the presence of the Dresselhaus [27] spin-orbit interaction in a zinc-blende structure, acting on the spin with its magnitude and orientation depending on \vec{k} , which results in spin precession (spin relaxation) with intrinsic Larmor frequency $\Omega_s(\vec{k}) = (e/m)\hbar(\vec{k})$ during the time between collisions.

The corresponding Hamiltonian (DP Hamiltonian) describing the precession of electrons in the conduction band is $H_{so}(\vec{k}) = (\hbar/2)\vec{\sigma}\cdot\Omega_s(\vec{k})$, where $\vec{\sigma}$ is the vector of Pauli spin matrices.

The increased electron momentum at higher electric fields brings about a stronger $\vec{h}(\vec{k})$ and consequently, the electron precession frequency $\Omega_s(\vec{k})$ becomes higher. The intrinsic magnetic field depends on the underlying material, on the geometry of the device, and on \vec{k} . Momentum-dependent spin precession described by the DP Hamiltonian, together with momentum scattering characterized by momentum relaxation time $\tau_p(E_{\vec{k}})$ leads to the DP spin relaxation.

Since the magnitude and the direction of \vec{k} changes in an uncontrolled way due to electron scattering with the environment, this process contributes to (DP) spin relaxation given by $1/(\tau_s)_{DP} = \gamma(\alpha/\hbar)^2 E_{\vec{k}}^3 / (E_g) \tau_p(E_{\vec{k}})$ [26], where $(\tau_s)_{DP}$ is the DP spin lifetime, $E_{\vec{k}} = k_B T_e$ and γ is a dimensionless factor that ranges from 0.8 to 2.7 depending on the dominant momentum relaxation process. During transport in the electric field, electrons are accelerated to higher velocities at higher fields, where the electron temperature T_e increases sharply due to the energy-independent nature of the dominant energy relaxation process

via the longitudinal polar optical phonon scattering [28]. The resulting high T_e leads to enhanced DP spin relaxation ($1/(\tau_s)_{DP} \propto T_e^3 \tau_p$) because they have large kinetic energy between successive collisions.

The main spin relaxation mechanisms for semiconductors discussed in the literature are the Elliot–Yafet (EY), Bir–Aronov–Pikus (BAP) and DP [3]. For GaAs, the EY spin relaxation is less effective due to the large E_g and low scattering rate. For n -doped materials, as holes are rapidly recombined with electrons due to the presence of a large number of electrons, spin relaxation due to the BAP mechanism is usually blocked [27]. The spin relaxation in n -doped GaAs is therefore dominated by the DP mechanism.

Conclusion

The optical AHE as a technique for the electrical detection of spin current in nonmagnetic semiconductors was observed. As no external magnetic field was used, the effect was without any contribution from the ordinary Hall current. The optical pure AHE was originated from nonequilibrium magnetization induced by spin-polarized electrons generated by the circularly polarized light. Bias-field and pumping photon energy dependences of the optical AHE were observed. However, it was demonstrated that when the electron spins were dragged with a high field a very significant decrease was occurred in the spin polarization due to an increase in the spin precession frequency of the hot electrons. The results were discussed based on the dominating spin relaxation mechanism in n -type semiconductors with a zinc-blende structure.

References

1. Spin Electronics, M. Ziese and M. J. Thornton, Eds., Vol. 569, Springer–Verlag, Heidelberg, 2001.
2. Semiconductor Spintronics and Quantum Computation, D.D. Awschalom, D. Loss, N. Samarth, Eds., Springer, Berlin, 2002.
3. I. Žutić, J. Fabian, S. D. Sarma, Fundamentals of spintronics: applications and devices, *Rev. Mod. Phys.* 76 (2004) 323.
4. D'yakonov, M.I., Khaetskii, A.V. Spin Hall Effect (Spin Physics in Semiconductors, M.I. D'yakonov, Ed., Springer-Verlag, Berlin, (2008).
5. M. Idrish Miah, Semiconductor spintronics and its requirements, *J. Optoelectron. Adv. Mater.* 10 (2008) 2487.
6. M. Idrish Miah, Spin drift-diffusion and its crossover in semiconductors, In: Spintronics: Materials, Applications and Devices (NS Publishers, New York, 2008).
7. J. M. Kikkawa and D. D. Awschalom, Resonant spin amplification in n -type GaAs, *Phys. Rev. Lett.* 80 (1998) 4313.
8. M. Idrish Miah, Diffusive to drift-diffusion crossover of spin transport in the low-field regime, *Appl. Phys. Lett.* 92, 092104 (2008) 092104. Also in *Virtual J. Nanoscale Sci. Technol.* 17 (11), March 17 (2008)
9. M. Idrish Miah, Two-photon spin-polarization spectroscopy in Si-doped GaAs, *J. Phys. Chem. B* 113, (2009) 6800.
10. M. Idrish Miah, Roles of the bias fields in the exchange interaction between the electron and hole spins in GaAs quantum wells, *Appl. Phys. Lett.* 94, 182106 (2009) 182106. Also in *Virtual J. Nanoscale Sci. Technol.* 19 (20), May 18 (2009).
11. M. Idrish Miah, Optical spin generation/detection and spin transport lifetimes, *Mater. Sci. Engineer. B* 176 (2011) 252.
12. M. Idrish Miah and E. MacA. Gray, Spin transport and spin current detection in semiconductors, *Solid State Sci.* 10 (2008) 205.
13. Y. Kato, R. C. Myers, A. C. Gossard, and D. D. Awschalom, Observation of the spin Hall effect in semiconductors, *Science* 306 (2004) 1910.
14. M. Idrish Miah, Drift-diffusion crossover and the intrinsic spin diffusion lengths, *J. Appl. Phys.* 103 (2008) 063718.
15. The Hall Effect and Its Applications, C. L. Chien, and C. R. Westgate, Eds. (Plenum, New York, 1980).
16. J.- N. Chazalviel, Spin-dependent Hall effect in semiconductors, *Phys. Rev. B* 11 (1975) 3918.
17. M. Idrish Miah, Observation of the anomalous Hall effect in GaAs, *J. Phys. D: Appl. Phys.* 40, (2007) 1659.
18. M. I. D'yakonov and V. I. Perel', Possibility of orienting electron spins with current, *JETP Lett.* 13 (1971) 467.

19. M. I. D'yakonov and V. I. Perel', Current-induced spin orientation of electrons in semiconductors, *Phys. Lett. A* 35 (1971) 459.
20. G. Lampel, Nuclear dynamic polarization by optical electronic saturation and optical pumping in semiconductors, *Phys. Rev. Lett.* 20 (1968) 491.
21. M. Idrish Miah, Low-temperature annealed ohmic contacts to Si-doped GaAs and contact formation mechanisms, *Mater. Chem. Phys.* 113 (2009) 967.
22. M. Idrish Miah and E. MacA. Gray, Inter-band transition effects in spin generation, *Curr. Opin. Solid State Mater. Sci.* 14 (2010) 49.
23. D. Hägele, M. Oestreich, W. W. Rühle, N. Nestle, and K. Eberl, Spin transport in semiconductors, *Appl. Phys. Lett.* 73 (1998) 1580.
24. H. Sanada, I. Arata, Y. Ohno, Z. Chen, K. Kayanuma, Y. Oka., F. Matsukura, and H. Ohno, The Second International Conference on Physics and Application of Spin Related Phenomena in Semiconductors, Würzburg, Germany, 2002.
25. M. Idrish Miah and I. V. Kityk, Band energy structure calculations and spin effect in zinc-blende semiconductors, *Opt. Commun.* 284 (2011) 2523.
26. G. E. Pikus, A. N. Titkov: In Optical Orientation, Modern Problems in Condensed Matter Science (F. Meier and B. P. Zakharchenya, Eds.), Vol. 8 (Elsevier, North-Holland, Amsterdam, 1984).
27. M. Idrish Miah, High field electron-spin transport and observation of the Dyakonov–Perel spin relaxation of drifting electrons in low temperature-grown gallium arsenide, *Phys. Lett. A* 372 (2008) 6981.
28. S. Adachi, GaAs and Related Materials: Bulk Semiconducting and Superlattice Properties (World Scientific, Singapore, 1994).

(2011) <http://www.jmaterenvironsci.com>